Article published online: 2023-03-15

Application of Chiral Piperidine Scaffolds in Drug Design

Qiu-Shi Chen[1,2] Jian-Qi Li[2] Qing-Wei Zhang[2,*]

[1] School of Chemistry and Chemical Engineering, Shanghai University of Engineering Science, Shanghai, People's Republic of China
[2] Shanghai Institute of Pharmaceutical Industry Co., Ltd., China State Institute of Pharmaceutical Industry, Shanghai, People's Republic of China

Address for correspondence Qing-Wei Zhang, PhD, Novel Technology Center of Pharmaceutical Chemistry, Shanghai Institute of Pharmaceutical Industry Co., Ltd., 285 Gebaini Road, Shanghai 201203, People's Republic of China (e-mail: sipiqingwei@163.com).

Pharmaceut Fronts 2023;5:e1–e14.

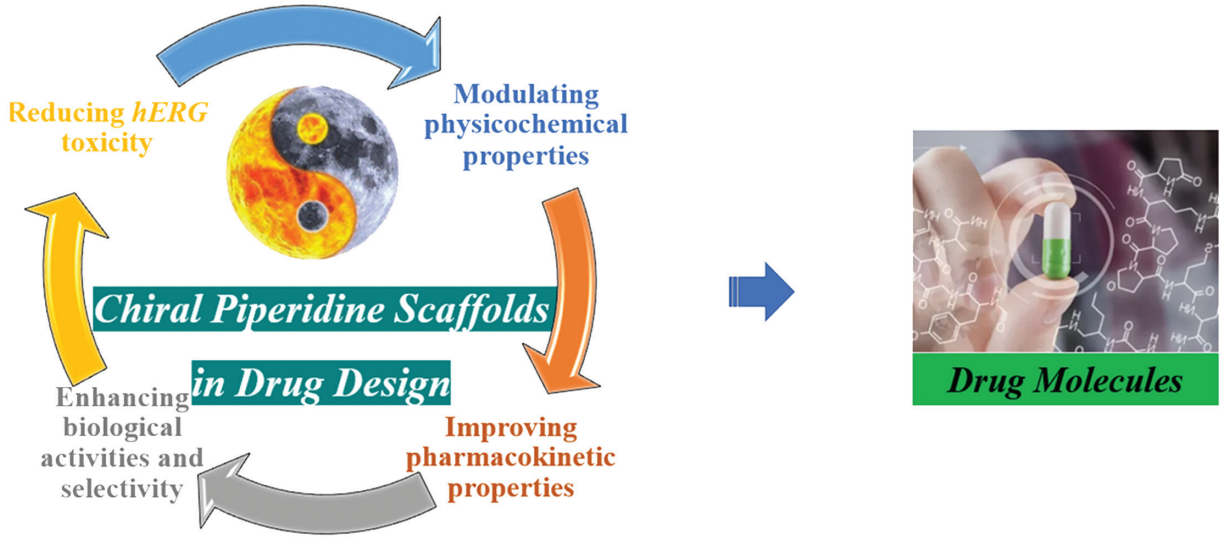

Abstract

Chiral piperidine scaffolds are prevalent as the common cores of a large number of active pharmaceuticals in medical chemistry. This review outlined the diversity of chiral piperidine scaffolds in recently approved drugs, and also covers the scaffolds in leads and drug candidates. The significance of chiral piperidine scaffolds in drug design is also discussed in this article. With the introduction of chiral piperidine scaffolds into small molecules, the exploration of drug-like molecules can be benefitted from the following aspect: (1) modulating the physicochemical properties; (2) enhancing the biological activities and selectivity; (3) improving pharmacokinetic properties; and (4) reducing the cardiac *hERG* toxicity. Given above, chiral piperidine-based discovery of small molecules will be a promising strategy to enrich our molecules' library to fight against diseases.

Keywords

- chiral piperidine scaffolds
- drug-like
- drug molecules
- drug design
- medicinal chemistry

received
July 28, 2022
accepted
January 26, 2023

DOI https://doi.org/10.1055/s-0043-1764218.
ISSN 2628-5088.

Georg Thieme Verlag KG, Rüdigerstraße 14, 70469 Stuttgart, Germany

Introduction

Chiral drugs has attracted more and more attention due to their perfect adaptability to protein-binding sites. The chiral state of a molecule can be achieved by introducing a chiral center to the structure, and owing to this fact, their druggability may be greatly influenced.[1] Piperidine, as a six-membered nitrogenous heterocyclic ring, is widely present in the structure of approved drugs.[2] Thus, the study of stereochemistry of piperidine scaffolds has attracted a great deal of interest since the late last century, and has become a hot topic recently.[3] According to the U.S. Food and Drug Administration data, there are 245 drugs approved from 2015 to June 2020, including small molecules and macromolecules. Among them, the number of chiral piperidine-containing drugs is nine, including avycaz (**1**), cotellic (**2**), varubi (**3**), zejula (**4**), daurismo (**5**), galafold (**6**), akynzeo (**7**), ubrelvy (**8**), and recarbrio (**9**) (►**Table 1**, ►**Fig. 1**).[4] Although the introduction of chiral centers in piperidine scaffolds is often associated with increased number of synthetic steps and unusual reaction procedures, and ultimately leads to an increase in synthesis effort,[5,6] medical researchers believe that the increased expenditure is worth because of the expected favorable effects on physicochemical properties, potency, selectivity, and pharmacokinetic (PK) profile that may be induced by the chiral piperidine scaffolds. Thus, this review aimed to provide a broad perspective on the latest advances of chiral piperidine scaffolds in medicinal chemistry. The study would assist drug discoverers to rationally design molecules for various diseases.

Application of Chiral Piperidine Scaffolds in Drug Design

Modulating the Physicochemical Properties

Physicochemical properties of a compound can be predicted by the parameters of pK_a, logD, and logP, and methods for improving the physicochemical properties of drugs include introducing hydrophilic or lipophilic groups, changing charge state and their spatial configurations to form intermolecular or intramolecular forces, etc.[7,8] The piperidine ring originally is a kind of groups with properties of both hydrophilicity and lipophilicity. The introduction of chiral centers in the piperidine ring, changing the position of a substituent, or introducing another substituent may alter its physicochemical properties effectively.

In 2012, Ndungu et al reported a series of measles virus RNA-dependent RNA polymerase (MeV-RdRp) inhibitors.[8] In their earlier work, they identified **10** as a potent and selective MeV-RdRp inhibitor, which exhibited an excellent activity

Table 1 The U.S. FDA-approved drugs that contain chiral piperidine moieties from 2015 to June 2020

Brand name	Indication	Year of approval	Sponsor	Target
Avycaz (Ceftazidime-avibactam/IV)	Intra-abdominal infections (cIAI), UTI	2015	Allergan	Ceftazidime: vell wall inhibitor; avibactam: non-β-lactamase inhibitor
Cotellic	Metastatic melanoma with a BRAF mutation (V600E or V600K)	2015	Genentech	MAPK
Varubi	Nausea and vomiting (emesis)	2015	Tesaro	Substance P/NK1 receptor antagonist
Zejula	The epithelial ovarian, fallopian tube, or primary peritoneal cancer	2017	Tesaro	PARP-1, 2, and 3 enzymes
Daurismo	AML	2018	Pfizer	Smoothened (Smo) receptor inhibitor: inhibits Hedgehog signaling pathway
Galafold	Fabry disease	2018	Amicus T herapeutics	Alpha-galactosidase A
Akynzeo (Fosnetupitant and Palonosetron/iv)	Chemotherapy-induced nausea and vomiting (emesis)	2018	Helsinn Group	Fosnetupitant: selective NK-1 receptor antagonist; Palonosetron: antagonist of 5-HT3 receptors
Ubrelvy	Migraine with or without aura in adults	2019	Allergan	CGRP receptor antagonist
Recarbrio (Imipenem, cilastatin, and relebactam/iv)	Urinary tract and abdominal infections	2019	Merck & Co.	Imipenem; inhibit cell-wall synthesis, cilastatin; inhibitor of renal dehydropeptidase, and relebactam; β-lactamase inhibitor

Abbreviations: AML, acute myeloid leukemia; UTI, urinary tract infection.

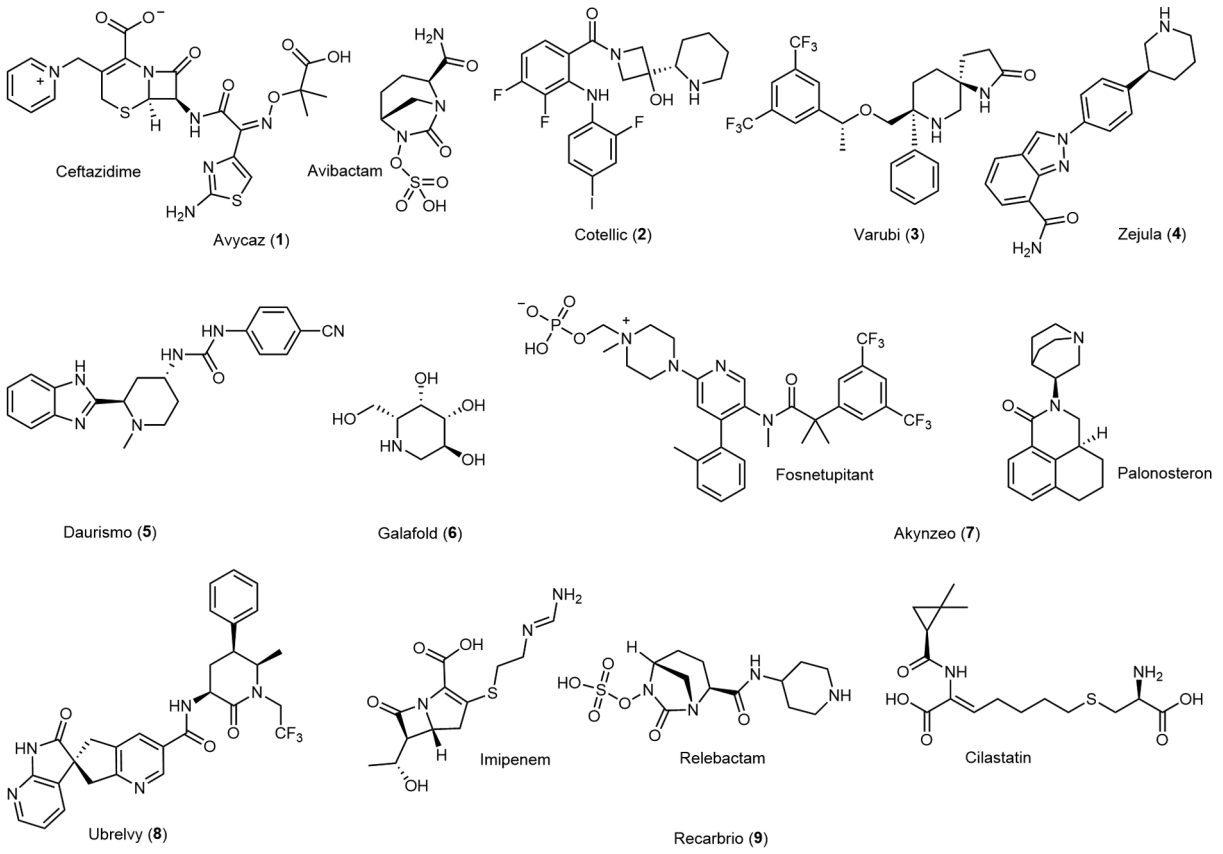

Fig. 1 Structure of the U.S. FDA-approved drugs that contain chiral piperidine moieties from 2015 to June 2020. FDA, Food and Drug Administration.

($EC_{50} = 14$ nmol/L) but suffered from poor water solubility and low oral bioavailability. Further structure–activity relationship (SAR) studies showed that introducing a substituent at the 2-position of the piperidine ring could effectively enhance the aqueous solubility of this series of compounds. Then, optimization of *in vivo* potency and aqueous solubility of compound **10** led to the discovery of compound **11**, which showed an improved aqueous solubility of 60 µg/mL and a maintained MeV-RdRp inhibition ($EC_{50} = 60$ nmol/L) (►**Fig. 2**).

SUCNR1 (succinate receptor 1, initially named GPR91) is a G-protein-coupled receptor, and identifies succinate as its endogenous ligand.[9] Succinate is responsible for ATP formation and energy supply,[10] and is normally located in the mitochondria, but under certain pathological conditions, it acts as a signaling molecule, and is recognized as a danger signal by SUCNR1.[10,11] In the process of exploring a new class of SUCNR1 inhibitors, Velcicky et al discovered that both 4-piperidyl analog (**12**) and 3-piperidyl analog (**13**) had a good SUCNR1 inhibition.[12] However, the logD (pH 7.4) values of the two compounds varied a lot (►**Table 2**), and compound **13** showed quite remarkable increase in the permeability and lipophilicity when compared with **12**. Further research

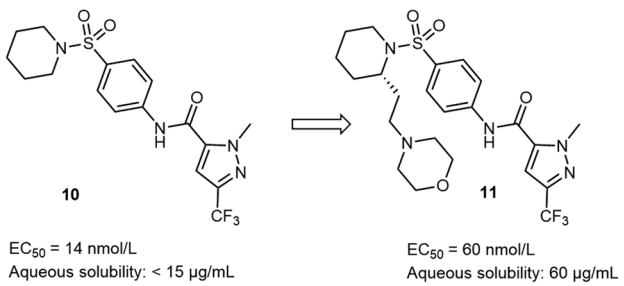

Fig. 2 The influence of the introduction of chiral center in piperidine ring on aqueous solubility of MeV-RdRp inhibitors.

Table 2 The influence of the introduction of chiral center in piperidine ring on logD of SUCNR1 inhibitors

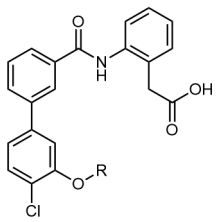

Compound	R	hSUCNR1 GTPγS (µmol/L)	logD7.4
12	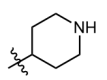	0.14	2.5
13	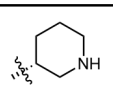	0.52	3.6

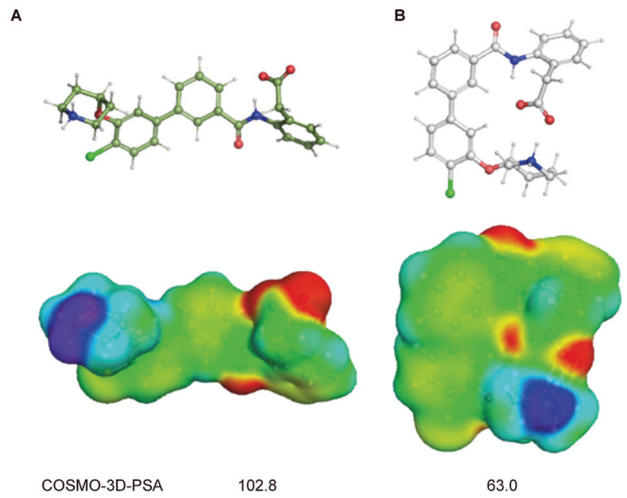

Fig. 3 Minimum-energy conformation in water at the TZVPD-FINE19 level for (A) **12** and (B) **13** (first row) and associated σ-surfaces (second row). The (*R*)-enantiomer was modeled for **13**. The folded conformation observed for **13** with the intramolecular salt bridge leads to a drastic reduction in the overall polar surface area as quantified by COSMO-3D-PSA.[13]

revealed that the two compounds populated remarkably different shapes in an aqueous solution (►**Fig. 3**).[13] Compound **12** preferred an elongated conformation, while compound **13** was folded with an intramolecular salt bridge formed between the piperidine and the carboxylic acid moieties.[12]

Influence on the Biological Activity

Improving the Biological Activity

Chiral centers are widely found in approved drugs and drug candidates, and have shown unique privileges in enhancing drug efficacy. Due to the asymmetry of organisms, the biological properties of chiral molecules are more abundant than achiral molecules.[14] Currently, the study of stereochemistry of the piperidine scaffold has fascinated chemists because of its profound effect on biological activity of a drug.[15] As is shown in a wide range of research studies, introducing a chiral center in the piperidine ring can not only provide researchers with more chiral piperidine-containing compounds, which is essential to improve the activity of the drugs, but also make the compound have more configurational isomers to fit in the cavum of protein.[15]

The mitogen-activated protein kinase (MAPK) signaling pathway has four branches. Among which, the extracellular regulated protein kinases (ERK) pathway plays an important role in the development of tumors.[16] In this pathway, there are three important target proteins, including Ras, Raf, and mitogen-activated protein (MEK). Many research studies suggested that inhibition of MEK may suppress the activation of ERK effectively, which is essential to the blockage of this pathway.[16,17] In the process of identifying a new series of MEK1/2 inhibitors, the imidazoquinoline core was considered, and Poddutoori et al discovered 1-(piperidin-4-yl)-1*H*-imidazo[4,5-*c*]quinoline (**14**) as a high-throughput screening hit, which had an acceptable MEK1/2 inhibition ($EC_{50} = 400$ nmol/L).[18] The structure-based design led to the discovery of analogue **15**, whose MEK1/2 inhibition is eightfold higher than **14**. Further optimization focused on the modification of the piperidine ring of **15**, with a fluorine introduced at the 3-position of the piperidine ring, to give chiral **16**, which exhibited a further improved potency ($EC_{50} = 5$ nmol/L) and aqueous solubility (logP = 1.6) as well as high oral bioavailability (*F*% = 65) (►**Fig. 4**). The crystal structure of MEK1 in complex with **16** revealed that the 3-substitued piperidine side chain can fit into the cavum of MEK easily, which is essential to increase the drug potency (►**Fig. 5**).

In exploration of a new series of CVF-Bb (Cobra Venom Factor binds factor B) inhibitors, Mainolfi et al discovered the significance of R groups on the potency of CVF-Bb inhibition of a compound (►**Table 3**).[19] When the R group is a morpholine ring or a piperidine ring with no chiral center, the potency was low. Taking compound **18** as an example, it had an IC_{50} value of 50 μmol/L; however, when a phenyl was introduced at 2-position of the piperidine ring of **18**, compound **19** was obtained, with a great increase in CVF-Bb inhibitory potency ($IC_{50} = 5.9$ μmol/L). Further optimization led to the discovery of **20** and **21**, whose potencies are approximately 170-fold higher than **19**. It is noteworthy that the introduction of an ethoxy group at the 4-position of the piperidine ring provided **21** with approximately twofold potency higher than **20**, which also proved the good effect of introducing a chiral center in the piperidine ring. Then, the replacement of methyl with a methoxy led to

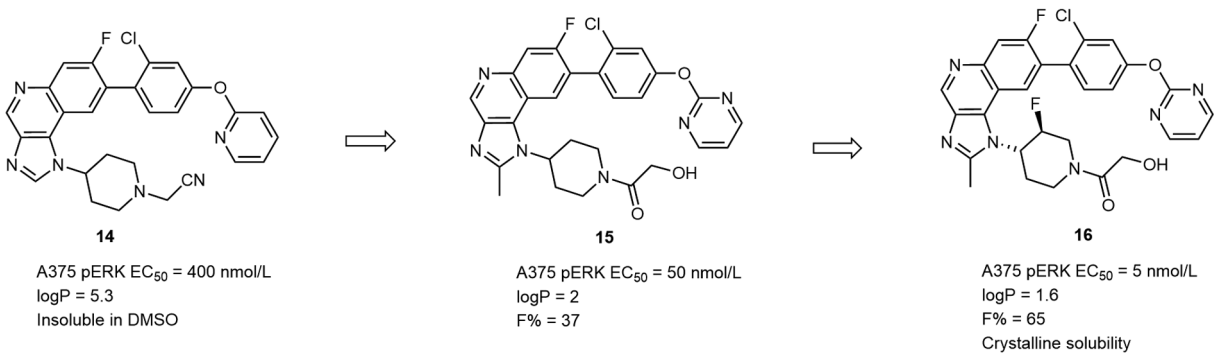

Fig. 4 The influence of the introduction of chiral center in piperidine ring on activities of MEK1/2 inhibitors.

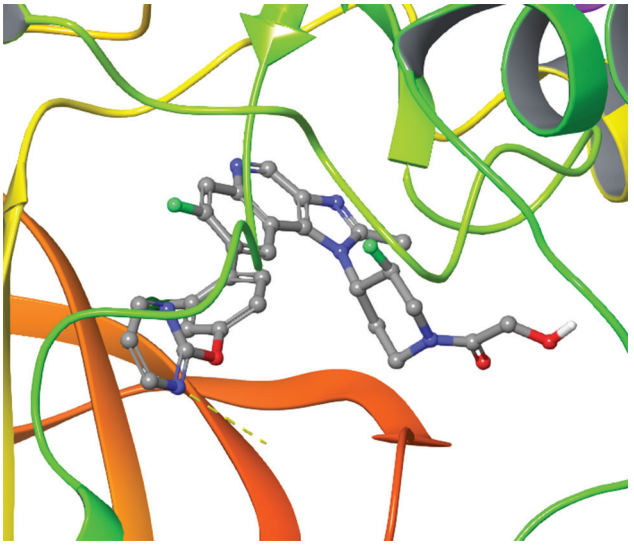

Fig. 5 Crystal structure of **16** bound to MEK1 (PDB code: 7PQV).[18]

22, whose potency was further increased and PK properties are good (►**Fig. 6**).

P53 is a kind of tumor suppressor protein that maintains the integrity of the genome in a cell.[20] Human double minute 2 (HDM2) is a ubiquitin protein ligase that negatively regulates p53 and lessens its transcriptional activity as well as promotes p53 protein degradation.[20,21] Disrupting the HDM2-p53 protein–protein interaction (PPI) with a small molecule has been recognized as a potential way in cancer therapies.[22] In 2014, Ma et al reported the discovery of a new series of HDM2-p53 PPI inhibitors.[21] Structure-based design led to the discovery of **23** that had a piperidine-containing core and an acceptable potency (IC_{50} = 169 nmol/L). Further optimization of **23** led to compound **24**, which was a potent HDM2-p53 PPI inhibitor (IC_{50} = 41 nmol/L) with an allyl at the 2-position of its piperidine ring. Compared with **23**, compound **24** showed an improved inhibition toward HDM2-p53 PPI and a favorable toxicity window between wt-p53 and mutant-p53 cell lines (►**Fig. 7**).

Table 3 The influence of R group on activities of CVF-Bb inhibitors

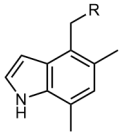

Compound	R	CVF-Bb IC_{50} (μmol/L)
17		>100
18		50
19	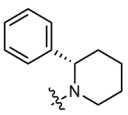	5.9
20	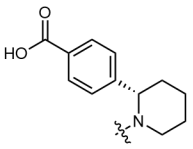	0.033
21	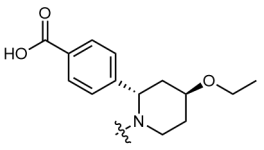	0.018

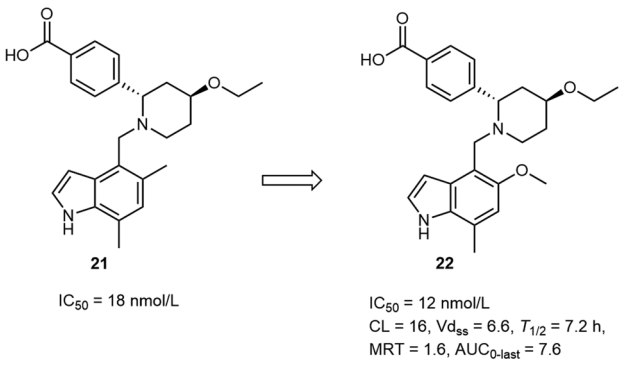

Fig. 6 The further optimization of **21**.

In 2017, Rutaganira et al reported the discovery of a new series of calcium-dependent protein kinase 1 (CDPK1) inhibitors.[23] Among which, compound **27** showed the best potency with an IC_{50} value of 10.9 nmol/L (compared with **25** and **26**, whose IC_{50} values are 14.15 and 77.5 nmol/L), suggesting an important role of two fluorine atoms at 3-position of the piperidine ring (►**Table 4**). Interestingly, **27** produced a chiral center at the 4-position of the piperidine ring. The skeleton of **27** fits well into the cavum (►**Fig. 8a**), observed by the crystal structure of CDPK1 in complex with **27** (PDB code: 5W9E), and the introduction of a chiral center made the nitrogen of the piperidine ring form two salt bridges with the GLU135 and GLU178 residues of CDPK1 (►**Fig. 8b**).

Glucagon-like peptide-1 receptor (GLP-1R) is the most important incretin in type-2 diabetes therapy. GLP-1R enhances the release of glucose-dependent insulin and suppresses the apoptosis of islet β cells.[24] However, the half-life

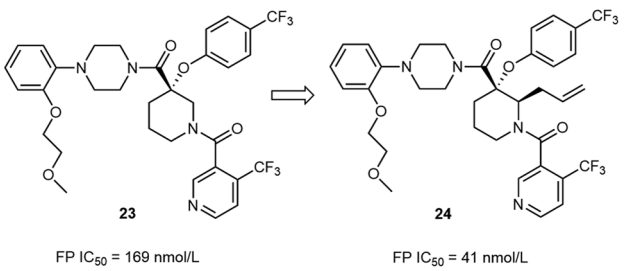

Fig. 7 The influence of the introduction of chiral center in piperidine ring on activities of HDM2-p53 PPI inhibitors.

Table 4 The influence of R group on activities of CDPK1 inhibitors

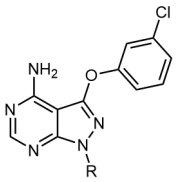

Compound	R	CDPK1 IC_{50} (nmol/L)
25	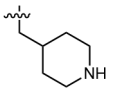	14.15
26	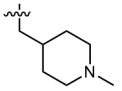	77.5
27	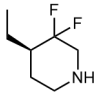	10.9

Table 5 The influence of the position and type of R group on activities of GLP-1R agonists

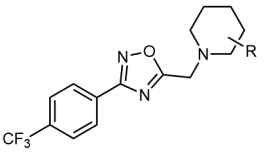

Compound	Position of substituent	R	Potentiation of GLP-1 E_{max} (%)
28	4	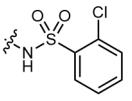	24 ± 7
29	2	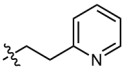	50 ± 8
30	3	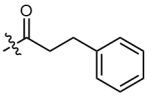	42 ± 6
31	3	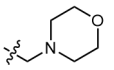	60 ± 7

time of this native peptide in blood is very low (1 – 2 minutes) as it can be mainly rapidly degraded by circulating dipeptidyl peptidase (DPP-4).[25] Therefore, it is of great importance to develop a potent GLP-1R agonist. In 2021, Decara et al discovered a new series of GLP-1R agonists that contain a 1,2,4-oxadiazole core and a substituted piperidine ring.[25] Among which, the position of the substituent on the piperidine ring mattered much to their activity. When a substituent is present at 4-position of the piperidine ring (**28**), a poor GLP-1 potentiation (E_{max} = 24%) was achieved. When the substituent is morpholine-1-methyl and at 3-position of the piperidine ring (**31**), the GLP-1 potentiation of the compound was increased to 60% (►**Table 5**).

In 2016, Humphreys et al reported the discovery of a series of p300/CBP and p300/CBP associated factor (PCAF) inhibitors that had a pyridazin-3(2*H*)-one core, among which, the type of R groups was of great significance to their

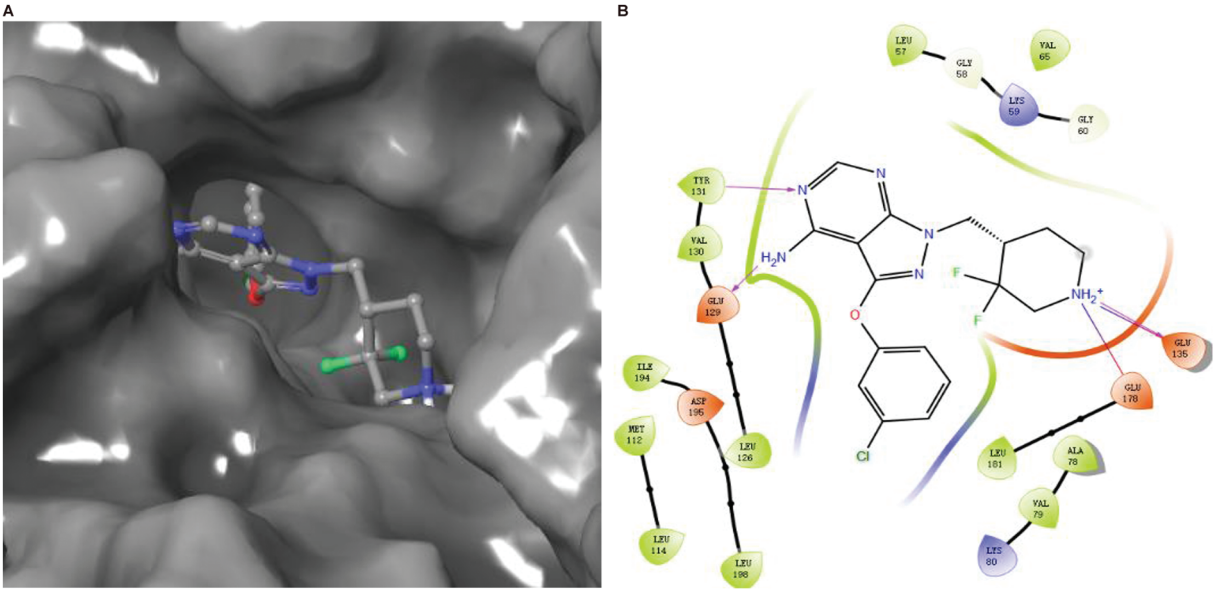

Fig. 8 (A) Crystal structure of **27** binding to CDPK1 (PDB code: 5W9E). (B) The interaction between **27** and CDPK1.[23]

Table 6 The influence of R group on activities of PCAF inhibitors

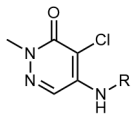

Compound	R	PCAF pIC_{50}
32		4.8
33	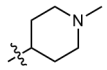	4.8
34		6.3

activities.[26] When the R group was a pyrrolidine (**32**) or a 4-substituted piperidine (**33**), the potencies of compounds were low. But when the substitution site in the piperidine ring changed from 4 to 3 (**34**), the potencies of compounds improved a lot (►**Table 6**). Further SAR research studies discovered that introducing a phenyl at 5-position of the piperidine ring can further increase its activity, which led to **35**, a potent PCAF inhibitor with a pIC_{50} value of 7.4 and exceptional selectivity over the bromodomain and extra-terminal domain (BET) bromodomain family (►**Fig. 9**).

In 2019, Huang et al discovered a series of PCAF inhibitors that had a similar structure to that of Humphreys et al.[27] The results also proved that the introduction of a chiral center in the piperidine ring improves the potencies of the series of compounds (►**Table 7**). As shown in ►**Table 7**, when the R group was a symmetric piperidine-containing structure (**36**, **37**, and **38**), the K_D values of the compounds were above 200 nmol/L. But when the substituent was at the 3- and 5-position of the piperidine ring (**39**), the K_D value increased to approximately 150 nmol/L. Further optimization led to **40**, a potent PCAF inhibitor that had similar structure to **39** and a further increased potency (►**Fig. 10**).

Cellular senescence exists widely in living beings, which has recently been considered as a potent strategy to suppress cancer progression.[28,29] In 2020, Oh et al reported the discovery of a new class of senescence-inducing small molecules with antimelanoma activities *in vitro*.[30] High-throughput screening and high-content screening led to the identification of compound **44**, a senescence inducer with good antimelanoma activities *in vitro*. SAR research studies suggested a great significance of the 1,3-substituent piperidine moiety in improving the potency of the compound. When the 1,3-disubstituent on the piperidine moiety was replaced by an azetidine (**41**), pyrrolidine (**42**), or symmetric piperidine (**43**) moiety, the activities of the compounds decreased a lot (►**Table 8**). Further modification focused on the replacement of the thiazole moiety, which led to the identification of **45** (►**Fig. 11**), a potent cellular senescence inducer with remarkable antimelanoma activity *in vitro* (EC_{50} = 40 nmol/L, IC_{50} = 30 nmol/L).

Table 7 The influence of R group on activities of PCAF inhibitors

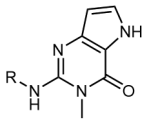

Compound	R	K_D (μmol/L)
36	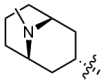	0.215
37	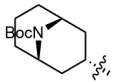	2.16
38	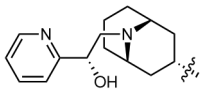	1.19
39	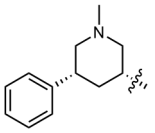	0.152

In 2014, Basarab et al reported a series of pyrrolamide topoisomerase II inhibitors.[31] Among them, compound **46** had a (piperidin-1-yl)thiazole-5-carboxylic acid moiety, and displayed DNA gyrase inhibitory potency and antibacterial activity toward gram-positive pathogens. Compound **46** functions by inhibiting the type II bacterial topoisomerases, DNA gyrase, and topoisomerase IV (Topo IV). To further

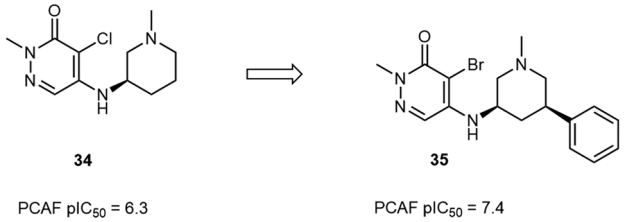

Fig. 9 The influence of the introduction of chiral center in piperidine ring on activities of PCAF inhibitors.

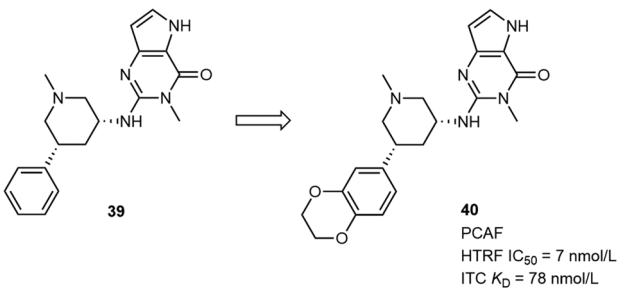

Fig. 10 The further modification of **39**.

Table 8 The influence of R group on activities of cellular senescence inducer

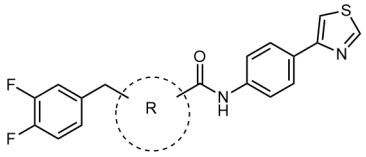

Compound	R	Activity (μmol/L)	
		EC_{50}	IC_{50}
41		> 20	> 20
42	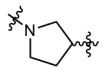	8.00	10.0
43	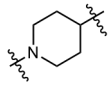	19.0	> 20
44	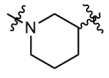	1.24	0.88

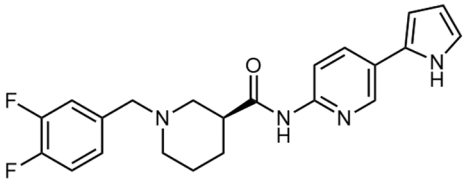

45
Senescence inducing activity EC_{50} = 40 nmol/L
Antiproliferative activity IC_{50} = 30 nmol/L

Fig. 11 The structure and *in vitro* activity of compound **45**.

improve its activity against topoisomerase II of bacteria, a methoxy group was introduced at 3-position of the piperidine ring to obtain **47**, which showed an improved inhibition to a wide range of gram-positive and gram-negative bacteria (►**Table 9**). Further modification was focused on the 4-position of the thiazole ring. For example, the introduction of (*S*)-((1-methoxypropan-2-yl)carbamoyl)thiazole-5-carboxylic acid unit led to **48**, which was proved to exhibit a further improved activity against bacterial growth.

Regulating the Target Selectivity of Drug Molecules

In 2018, Karlsson et al identified a series of new fibrinolysis inhibitors.[32] They found that introducing a chiral center in the piperidine ring of the series of compounds can effectively increase their selectivity over GABAa (►**Table 10**). Structure-based virtual screen led to the piperidinyl-substituted isoxazol-3-ol **49**, a fibrinolysis inhibitor with high potency but low selectivity over GABAa. Further research led to **50** that had a methyl at the 2-position of the piperidine ring. As is shown in ►**Table 10**, the potency of **50** decreased but the selectivity over GABAa remarkably increased. Then, the methyl group at 2-position of the piperidine ring was replaced by a neopentyl to give **51**, which had a further increased potency, yet maintained selectivity over GABAa.

In 2019, Shen et al reported the identification of a new series of $EGFR^{L858R/T790M/C797S}$ inhibitors.[33] They discovered that the type of R groups was of great significance to their selectivity over $EGFR^{WT}$. When the R group is a cyclohexanamine-containing moiety (**52** and **53**) or a symmetrical piperidine moiety (**54**), the selectivity of this series of compounds was low. But when the site of substitution was changed from 4-position to 3-position, their selectivity over $EGFR^{WT}$ increased remarkably (**55**, ►**Table 11**). At last, a fluorine substituent was introduced at 3-position of the phenyl and its potency was further increased (**56**, ►**Fig. 12**).

Improving PK Properties of Drug Molecules

Absorption, distribution, metabolism, and excretion properties are key indexes evaluating the druggability of drugs.

Table 9 The influence of introducing chiral center on piperidine ring on the activities of topoisomerase II inhibitors

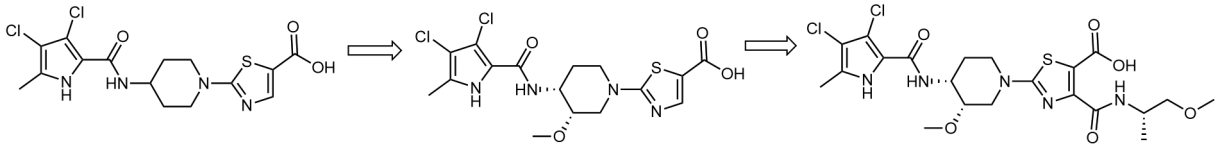

46 **47** **48**

Compound	Sau GyrB IC_{50} (nmol/L)	Eco ParE IC_{50} (nmol/L)	MICs (μg/mL)							
			Spn	Spy	MSSA	MRQR Sau	Hin	Mca	Eco	Eco *tolC*
46	<10	160	0.810	0.790	11.000	13.000	0.50	2.200	>64	0.22
47	<10	240	0.016	ND	0.320	0.500	0.18	0.031	64	0.18
48	<10	73	0.016	0.014	0.036	0.057	0.13	<0.008	24	0.94

Abbreviations: Eco, *E. coli*; Hin, *H. influenzae*; Mca, *M. catarrhalis*; MRQR Sau, methicillin resistant, quinolone resistant *S. aureus*; MSSA, methicillin sensitive *S. aureus*; ND, not determined; Spn, *S. pneumonia*; Spy, *S. pyogenes*.

Table 10 The influence of introducing chiral center on piperidine ring on the activities of fibrinolysis inhibitors

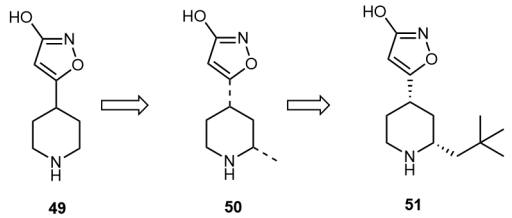

Compound	Clot lysis IC_{50} (μmol/L) (Hu plasma)	GABAa IC_{50} (μmol/L)
49	0.80	35
50	2.10	>2,000
51	0.44	>2,000

Piperidine rings, especially chiral piperidine rings, are usually introduced to improve PK properties (e.g., half-life, clearance, bioavailability) of a drug, and thus a common structural unit existing in drugs.[34]

Bruton's tyrosine kinase (BTK), a member of the Tec family of nonreceptor cytoplasmic tyrosine kinases, plays an essential role in B cell receptor signaling pathways and Fcγ receptor signaling in leukocytes.[35] BTK participated in the regulating of pathways that contribute to rheumatoid arthritis (RA), a multifactorial autoimmune disease.[36] In 2019, Watterson et al reported the discovery of Branebrutinib (**60**, ►**Fig. 13**), which is an irreversible BTK inhibitor, and currently in phase II clinical trials for the treatment of RA.[37] It is derived from the earlier described reversible BTK inhibitor BMS-986142 (**57**, ►**Fig. 13**) whose quinazolinedione ring system provides two bridging hydrogen bonds with Cys481 and Gln412 through two ordered water molecules.[37] To get a covalent, irreversible BTK inhibitor, they first replaced the quinazolinedione ring with a simple acrylamide acceptor and simplified the hexahydro carbazole core to the 2,3-dimethylindole ring system to achieve compound **58** (BTK $IC_{50} = 0.17$ nmol/L, Romas cell $IC_{50} = 16$ nmol/L; ►**Fig. 13**). However, **58** had a poor plasma PK in a mouse model, and this may be possibly due to the high acrylamide reactivity of the compound with thiols such as glutathione. Thus, alternation of accepters makes less contribution to resolving PK issue while sustaining the desirable potency. Therefore, the *N*-phenylacrylamide linker should be changed. Considering the balance between potency, electrophile reactivity, and PK profile, an *S*-3-piperidine appended with a but-2-ynamide accepter was introduced into the compound and gave **59** (►**Fig. 13**), a covalent BTK inhibitor with acceptable plasma concentrations *in vivo* but decreased potency (BTK $IC_{50} = 0.52$ nmol/L, Romas cell $IC_{50} = 40$ nmol/L). At last, a fluoro was introduced at the C5-position of the dimethylindole core and gave branebrutinib (**60**), which demonstrated improved potency (BTK $IC_{50} = 0.1$ nmol/L, Ramos cell $IC_{50} = 7.2$ nmol/L) and BTK inactivation rate (3.5×10^{-4} $nmol/L^{-1} \cdot min^{-1}$). The cocrystal structure of **60** binding to BTK showed that its chiral piperidine linker fit into the cavum of BTK well and the but-2-ynamide accepter formed a covalent bond with Cys481 (►**Fig. 14**). Further evaluation showed that the fluorine-substituted analogue **60** had a desirable safety and tolerability profile (►**Table 12**), and finally, **60** was advanced for clinical evaluation.

Table 11 The influence of R group on activities of $EGFR^{L858R/T790M/C797S}$ inhibitors

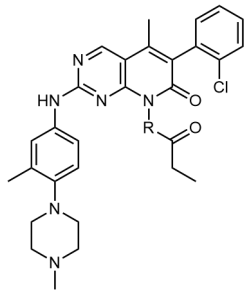

Compound	R	Kinase inhibition IC_{50} (nmol/L)	
		$EFGR^{WT}$	$EFGR^{TM}$
52	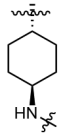	180.9 ± 80.8	519.9 ± 83.4
53	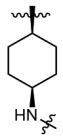	168.8 ± 63.4	27.7 ± 10.3
54	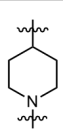	280.5 ± 0	866.9 ± 146.4
55	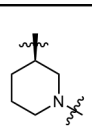	>1,000	65.1 ± 22.7

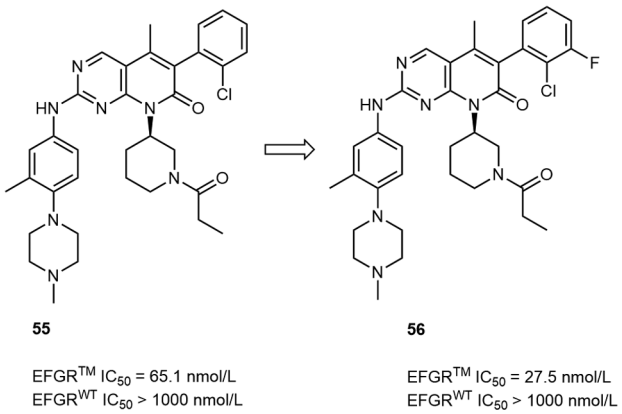

Fig. 12 The further optimization of **55**.

Checkpoint kinase 1 (CHK1) is a kind of Ser/Thr protein kinases that mediate the cellular response to DNA damage.[38] CHK1 inhibitors have been identified as potential cancer

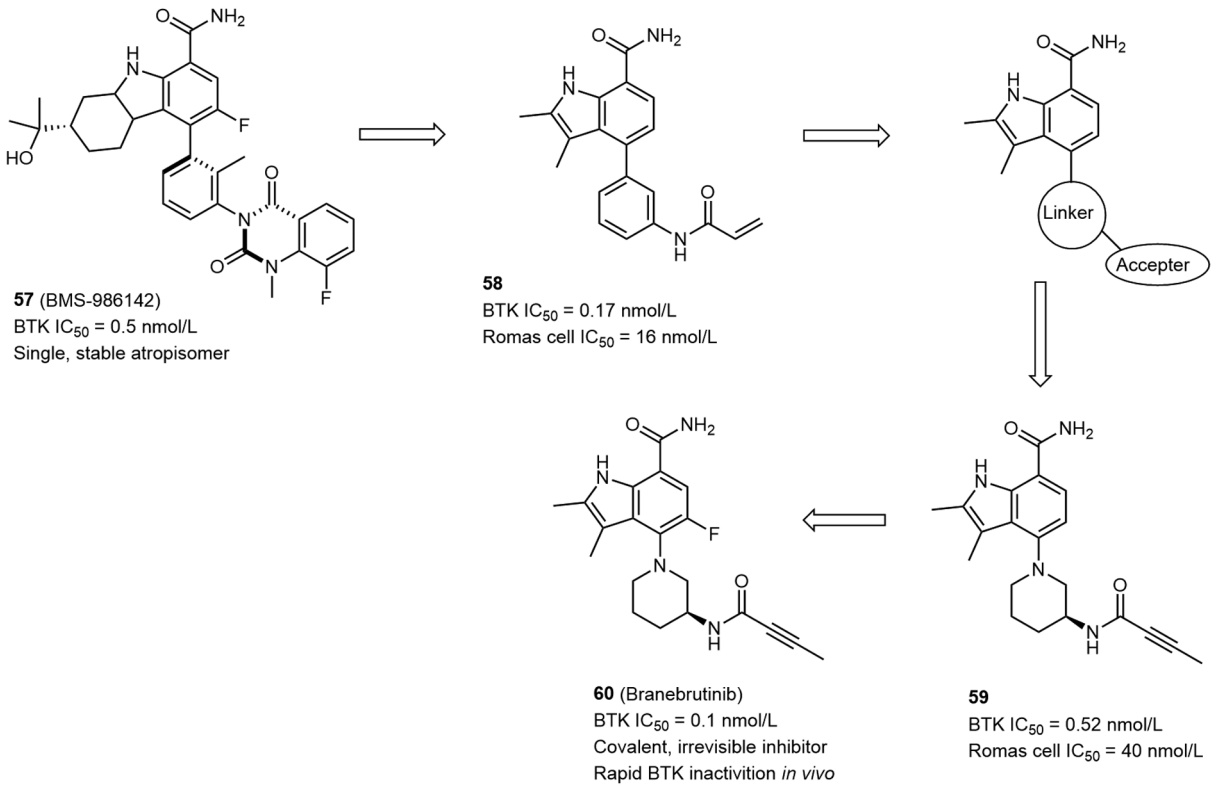

Fig. 13 Summary of the discovery of branebrutinib (**60**).

therapeutics, and had gained substantial interest from both academia and industry. In 2017, Yang et al reported the discovery of a series of CHK1 inhibitors.[38] In their previous work, the compound (**61**) with a 7-carboxamide thienopyridine core and a piperidine side chain was explored, which had a good potency but suffered from short half-life. Further SAR experiments showed that introducing a methyl at 2-position of the piperidine ring can effectively prolong its half-life. This led to the discovery of **62**, a potent CHK1 inhibitor with good potency and PK properties both *in vitro* and *in vivo* (►**Table 13**).

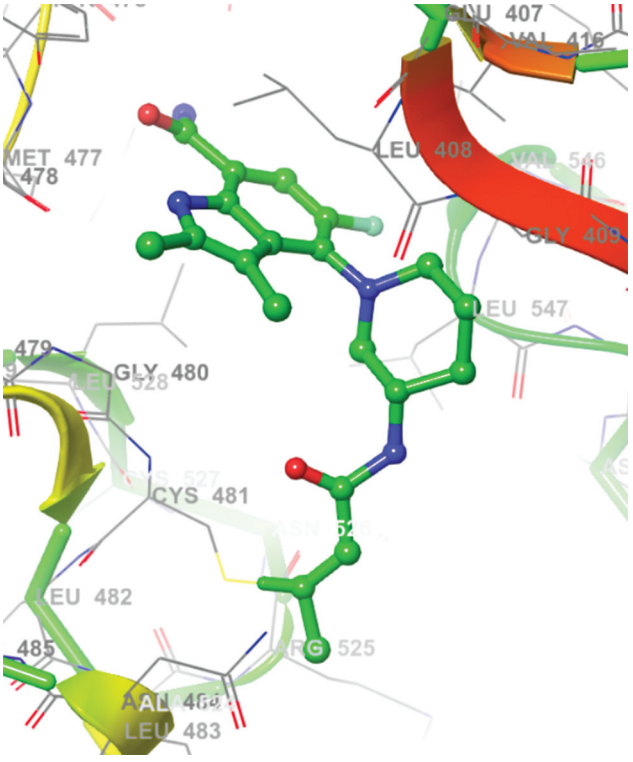

Fig. 14 Crystal structure of branebrutinib (**60**) bound to BTK (PDB code: 6O8I).[37]

In the process of identifying a new series of platelet-derived growth factor receptor (PDGFR) inhibitors, Hicken et al reported the discovery of **64**, a piperidine-containing PDGFR inhibitor with excellent potency and PK properties.[39] Structure-based design led to the discovery of **63**, which had satisfied potency and selectivity. However, **63** suffers from poor oral exposure and bioavailability. Further SAR study of **63** revealed that introducing a fluorine substituent at 3-position of the piperidine ring can effectively improve the PK properties of this series of compounds, which led to the discovery of **64**. Compared with **63** which has a symmetrical piperidine ring, **64** has an asymmetric piperidine ring with a fluorine substituent at the 3-position which enables its good oral exposure and bioavailability (►**Table 14**).

Reducing hERG Toxicity

hERG, the abbreviation of "human-ether-a-go-go-related gene," is a gene encoding a cardiac potassium channel whose protein product is the inner pore-forming part of a key membrane-bound potassium channel in myocardial tissue.[40] When the compound binds to the hERG potassium channel, the outflow of potassium ions is blocked and the

Table 12 Pharmacokinetic parameters of compound 60

Parameter	Mouse	Rat	Monkey	Dog
po dose (mg/kg)	4	5	2	2
iv dose	2	5	1	1
C_{max} (μmol/L), po	7.7	9.6 ± 1.0	2.3 ± 1.5	19 ± 2.5
T_{max} (μmol/L), po	1.0	0.58 ± 0.4	1.0 ± 0.3	0.67 ± 0.3
AUC (μmol/L·h), po	14	18 ± 0.8	4.9 ± 3.1	78 ± 3.0
$T_{1/2}$ (h), iv	0.46	4.3 ± 0.5	3.2 ± 2.5	3.0 ± 0.3
MRT (h), iv	0.57	0.80 ± 0.2	1.0 ± 0.4	4.1 ± 0.7
CL ($mL \cdot min^{-1} \cdot kg^{-1}$), iv	14	8.7 ± 0.4	9.4 ± 3.7	0.94 ± 0.25
V_{ss} (L/kg), iv	0.48	0.40 ± 0.1	0.45 ± 0.1	0.24 ± 0.11
F_{po} (%)	106	74 ± 3	46 ± 18.0	81 ± 18

Abbreviations: AUC, area under the concentration–time curve extrapolated to infinity; CL, total clearance; C_{max}, maximum plasma concentration; iv, intravenous injection; MRT, mean residence time; po, oral; $T_{1/2}$, elimination half-life; T_{max}, time to reach maximum concentration; V_{ss}, volume at steady state.

Table 13 The influence of the introduction of chiral center in piperidine ring on half-life time of CHK1 inhibitors

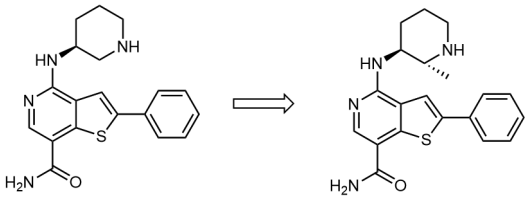

61 62

Compound	CHK1 IC_{50} (nmol/L)	$T_{1/2}$ (h)		
		Mouse	Rat	Dog
61	7	1.5	3.1	5.4
62	6	3.4	5.1	9.4

repolarization time of cardiomyocytes is prolonged, which may induce a fatal risk of torsades de pointes.[41,42]

With a wider and deeper knowledge of interaction between hERG inhibitors and their action site, possible strategies for decreasing drugs' hERG affinity have been focused, which include adjusting drug flexibility,[43] changing the charge state,[44] decreasing the pK_a,[45] and decreasing the lipophilicity.[45] Originally, the piperidine ring is a kind of structure with high lipophilicity, and usually has higher hERG inhibition than other groups.[46] Introducing a chiral center into the piperidine ring, either changing the position of a substituent or introducing another substituent, would help in decreasing hERG affinity, because by which, the spatial configuration of the compound may be changed, in parallel with a decreased pK_a, increased hydrophilicity, as well as modified polarity.

Uprosertib (**65**, also known as GSK-795) is a kind of protein kinase B (Akt) inhibitor identified by GlaxoSmithKline, and showed activities toward Akt1/2/3.[47] In 2019, Dong et al reported a new series of Akt1 inhibitors, which were based on the structure of uprosertib, and additionally introduced a piperidine moiety.[48] The connection between the primary amine moiety and the α-position of phenyl led to **66**, a potent Akt1 inhibitor with an IC_{50} value of 3 nmol/L but low hERG selectivity. Further optimization was focused on the

Table 14 The influence of introducing chiral center on piperidine ring on pharmacokinetic parameter of PDGFR inhibitors

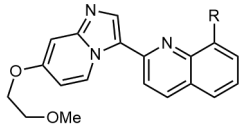

Compound	R	PDGFRβ cell IC_{50} (nmol/L)	1 mg/kg, iv		10 mg/kg, po		
			CL (mL/min/kg)	ER	AUC (μg)(h)/mL	C_{max} (μg/mL)	F (%)
63	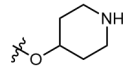	3	33	48	0.80	0.07	16
64	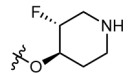	3	20	29	2.3	0.16	28

Abbreviations: AUC, area under the concentration–time curve extrapolated to infinity; CL, total clearance; C_{max}, maximum plasma concentration.
Note: Values were measured in male rat.

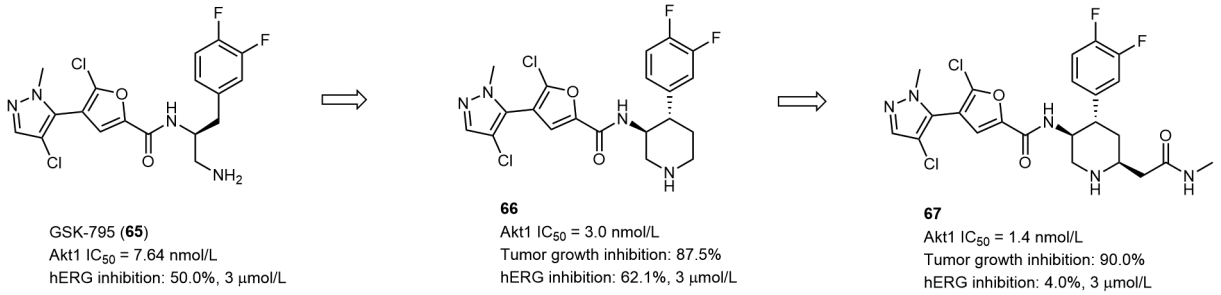

Fig. 15 The influence introducing chiral center on piperidine ring on hERG selectivity of Akt1 inhibitors.

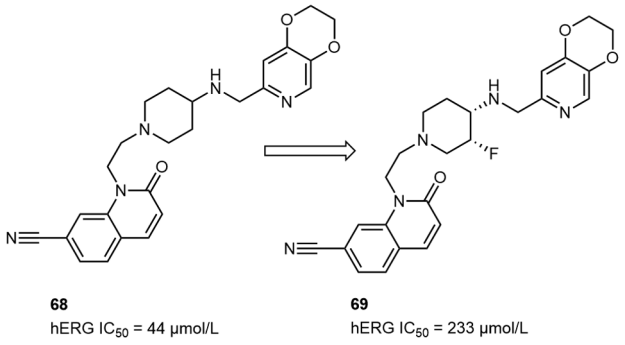

Fig. 16 The influence of introducing chiral center on piperidine ring on hERG selectivity of topoisomerase II inhibitors.

modification of its piperidine moiety, which led to **67**, an Akt1 inhibitor with even better potency and a higher hERG selectivity (►**Fig. 15**).

In 2012, Reck et al reported a series of aminopiperidine-containing compounds targeting bacterial type II topoisomerases (DNA gyrase and topo-isomerase IV).[49] In their work, the quinolinone carbonitrile derivative **68** was found to have a potent antibacterial activity, but suffered from hERG inhibition (hERG $IC_{50} = 44$ μmol/L) and QT prolongation *in vivo*. Introducing electron-withdrawing substituents such as hydroxy, methoxy, and fluoro groups at 3-position of the piperidine moiety could reduce the pK_a value of this series of compounds, and led to the subsequent hERG inhibition through reduction of binding affinity. Compound **69**, a *cis*-fluoro-substituted analogue, exhibited an improved selectivity over hERG ($IC_{50} = 233$ μmol/L) and a maintained potency toward gram-positive organisms (►**Fig. 16**). With good inhibition to bacterial growth and high hERG selectivity, **69** was selected as the candidate compound for a deeper preclinical study.

Renin, an aspartic protease, cleaves angiotensinogen to release inactive peptide angiotensin I (Ang-I) and controls the first and rate-limiting step of the renin–angiotensin–aldosterone system.[50] Blockade of renin has been considered as a useful method to treat hypertension and to protect from end-organ damage.[51] In 2014, Ehara et al identified a new class of renin inhibitors.[52] Compound **70**, a racemic *cis*-configured 3,5-disubstituted piperidine with weak renin inhibition, was discovered from a piperidine-based combinatorial library through high-throughput screens. Guided by structure-based design, researchers discovered **71**, whose activity was improved a lot but the hERG selectivity was low. Further modification was focused on improving hERG selectivity of this series of compounds. By introducing an (*R*)-configured hydroxyl at 4-position of the piperidine ring, **72** showed a higher renin inhibition and, most importantly, a good hERG selectivity with a hERG IC_{50} value of above 30 μmol/L (►**Fig. 17**).

Conclusion

Chiral piperidine scaffolds can be used to alter structure patterns with normal orientation, and have fascinated chemists for exploring desired molecules in medicinal chemistry. Due to distinctive three dimensionality that chiral centers impart, chiral piperidine scaffolds usually exhibit good adaptation to the binding site of the protein, resulting in the enhancement in activity and selectivity as well as fewer off-target effects.[53] Besides, π–π stacking interaction of a molecule may be reduced by the introduction of a chiral piperidine ring, thus, drug solubility and PK properties will be improved.[54] Furthermore,

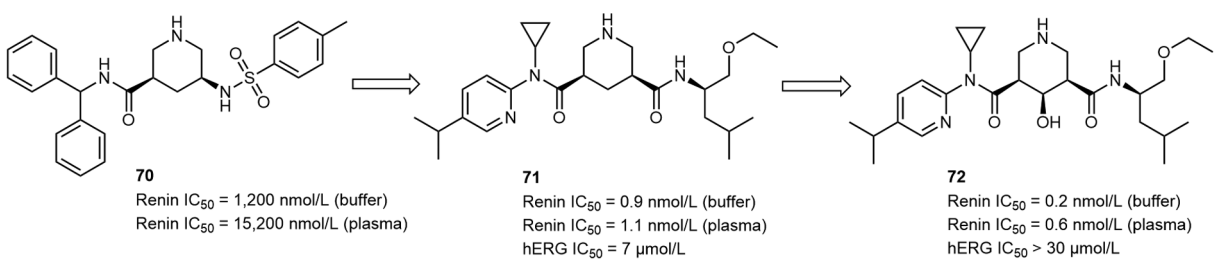

Fig. 17 The influence of introducing chiral center on piperidine ring on hERG selectivity of renin inhibitors.

chiral piperidine rings were also associated with good hERG selectivity, and this may be due to the modification of polarity and lipophilicity of a molecule.[55] Taken together, chiral piperidine rings are a powerful tool for medicinal chemists to expand novel structures in the current drug discovery.

Funding

We gratefully acknowledge financial supports from the National Science and Technology Major Project (Grant No. 2018ZX09711002-002-009), the National Natural Science Foundation of China (Grant No. 81703358), the Science and Technology Commission of Shanghai Municipality (Grant No. 17431903900, 18QB1404200, 21S11908000, 22ZR1460300), and the Graduate Innovation Fund Project of China State Institute of Pharmaceutical Industry (Grant No. YJS2021013, YJS2021011).

Conflict of Interest

The authors declare no conflict of interest.

Reference

1 Laplante SRD, D Fader L, Fandrick KR, et al. Assessing atropisomer axial chirality in drug discovery and development. J Med Chem 2011;54(20):7005–7022
2 Vitaku E, Smith DT, Njardarson JT. Analysis of the structural diversity, substitution patterns, and frequency of nitrogen heterocycles among U.S. FDA approved pharmaceuticals. J Med Chem 2014;57(24):10257–10274
3 Silvestri IP, Colbon PJJ. The growing importance of chirality in 3D chemical space exploration and modern drug discovery approaches for Hit-ID: topical innovations. ACS Med Chem Lett 2021;12(08):1220–1229
4 Bhutani P, Joshi G, Raja N, et al. U.S. FDA approved drugs from 2015-June 2020: a perspective. J Med Chem 2021;64(05):2339–2381
5 Kumorkiewicz-Jamro A, Świergosz T, Sutor K, Spórna-Kucab A, Wybraniec S. Multi-colored shades of betalains: recent advances in betacyanin chemistry. Nat Prod Rep 2021;38(12):2315–2346
6 Shan C, Xu J, Cao L, et al. Rapid synthesis of α-chiral piperidines via a highly diastereoselective continuous flow protocol. Org Lett 2022;24(17):3205–3210
7 Akamatsu M. Importance of physicochemical properties for the design of new pesticides. J Agric Food Chem 2011;59(07):2909–2917
8 Ndungu JM, Krumm SA, Yan D, et al. Non-nucleoside inhibitors of the measles virus RNA-dependent RNA polymerase: synthesis, structure-activity relationships, and pharmacokinetics. J Med Chem 2012;55(09):4220–4230
9 de Castro Fonseca M, Aguiar CJ, da Rocha Franco JA, Gingold RN, Leite MF. GPR91: expanding the frontiers of Krebs cycle intermediates. Cell Commun Signal 2016;14:3
10 Haas R, Cucchi D, Smith J, Pucino V, Macdougall CE, Mauro C. Intermediates of metabolism: from bystanders to signalling molecules. Trends Biochem Sci 2016;41(05):460–471
11 Tannahill GM, Curtis AM, Adamik J, et al. Succinate is an inflammatory signal that induces IL-1β through HIF-1α. Nature 2013; 496(7444):238–242
12 Velcicky J, Wilcken R, Cotesta S, et al. Discovery and optimization of novel SUCNR1 inhibitors: design of zwitterionic derivatives with a salt bridge for the improvement of oral exposure. J Med Chem 2020;63(17):9856–9875
13 Udvarhelyi A, Rodde S, Wilcken R. ReSCoSS: a flexible quantum chemistry workflow identifying relevant solution conformers of drug-like molecules. J Comput Aided Mol Des 2021;35(04): 399–415
14 Nadimetla DN, Al Kobaisi M, Bugde ST, Bhosale SV. Tuning achiral to chiral supramolecular helical superstructures. Chem Rec 2020; 20(08):793–819
15 Lovering F, Bikker J, Humblet C. Escape from flatland: increasing saturation as an approach to improving clinical success. J Med Chem 2009;52(21):6752–6756
16 Wu S, Cai W, Shi Z, et al. Knockdown of MTHFD2 inhibits proliferation and migration of nasopharyngeal carcinoma cells through the ERK signaling pathway. Biochem Biophys Res Commun 2022;614:47–55
17 Xing M, Yang Y, Huang J, et al. TFPI inhibits breast cancer progression by suppressing ERK/p38 MAPK signaling pathway. Genes Genomics 2022;44(07):801–812
18 Poddutoori R, Aardalen K, Aithal K, et al. Discovery of MAP855, an efficacious and selective MEK1/2 inhibitor with an ATP-competitive mode of action. J Med Chem 2022;65(05):4350–4366
19 Mainolfi N, Ehara T, Karki RG, et al. Discovery of 4-((2*S*,4*S*)-4-ethoxy-1-((5-methoxy-7-methyl-1*H*-indol-4-yl)methyl)piperidin-2-yl)benzoic acid (LNP023), a factor B inhibitor specifically designed to be applicable to treating a diverse array of complement mediated diseases. J Med Chem 2020;63(11):5697–5722
20 Calderon-González KG, Medina-Medina I, Haronikova L, et al. Cryptic in vitro ubiquitin ligase activity of HDMX towards p53 is probably regulated by an induced fit mechanism. Biosci Rep 2022; 42(07):BSR20220186
21 Ma Y, Lahue BR, Gibeau CR, et al. Pivotal role of an aliphatic side chain in the development of an HDM2 inhibitor. ACS Med Chem Lett 2014;5(05):572–575
22 Vassilev LT, Vu BT, Graves B, et al. In vivo activation of the p53 pathway by small-molecule antagonists of MDM2. Science 2004; 303(5659):844–848
23 Rutaganira FU, Barks J, Dhason MS, et al. Inhibition of calcium dependent protein kinase 1 (CDPK1) by pyrazolopyrimidine analogs decreases establishment and reoccurrence of central nervous system disease by Toxoplasma gondii. J Med Chem 2017;60(24):9976–9989
24 Graaf Cd, Donnelly D, Wootten D, et al. Glucagon-like peptide-1 and its class B G protein-coupled receptors: a long march to therapeutic successes. Pharmacol Rev 2016;68(04):954–1013
25 Decara JM, Vázquez-Villa H, Brea J, et al. Discovery of V-0219: a small-molecule positive allosteric modulator of the glucagon-like peptide-1 receptor toward oral treatment for "diabesity". J Med Chem 2022;65(07):5449–5461
26 Humphreys PG, Bamborough P, Chung CW, et al. Discovery of a potent, cell penetrant, and selective p300/CBP-associated factor (PCAF)/general control nonderepressible 5 (GCN5) bromodomain chemical probe. J Med Chem 2017;60(02):695–709
27 Huang L, Li H, Li L, et al. Discovery of pyrrolo[3,2- d]pyrimidin-4-one derivatives as a new class of potent and cell-active inhibitors of P300/CBP-associated factor bromodomain. J Med Chem 2019; 62(09):4526–4542
28 Lee S, Lee JS. Cellular senescence: a promising strategy for cancer therapy. BMB Rep 2019;52(01):35–41
29 Lee S, Schmitt CA. The dynamic nature of senescence in cancer. Nat Cell Biol 2019;21(01):94–101
30 Oh S, Kwon DY, Choi I, et al. Identification of piperidine-3-carboxamide derivatives inducing senescence-like phenotype with antimelanoma activities. ACS Med Chem Lett 2021;12 (04):563–571
31 Basarab GS, Hill PJ, Garner CE, et al. Optimization of pyrrolamide topoisomerase II inhibitors toward identification of an antibacterial clinical candidate (AZD5099). J Med Chem 2014;57(14): 6060–6082
32 Karlsson S, Pettersen D, Sörensen H. AZD6564, discovery of a potent 5-substituted isoxazol-3-ol fibrinolysis inhibitor and development of an enantioselective large-scale route for its preparation. ACS Symposium Series 2018;1307:151–184

33 Shen J, Zhang T, Zhu SJ, et al. Structure-based design of 5-methylpyrimidopyridone derivatives as new wild-type sparing inhibitors of the epidermal growth factor receptor triple mutant ($EGFR^{L858R/T790M/C797S}$). J Med Chem 2019;62(15):7302–7308

34 Zhang X, Sheng X, Shen J, et al. Discovery and evaluation of pyrazolo [3,4-*d*]pyridazinone as a potent and orally active irreversible BTK inhibitor. ACS Med Chem Lett 2019;11(10):1863–1868

35 Tichenor MS, Wiener JJM, Rao NL, et al. Discovery of JNJ-64264681: a potent and selective covalent inhibitor of Bruton's tyrosine kinase. J Med Chem 2022;65(21):14326–14336

36 Liu J, Guiadeen D, Krikorian A, et al. Discovery of 8-amino-imidazo [1,5-a]pyrazines as reversible BTK inhibitors for the treatment of rheumatoid arthritis. ACS Med Chem Lett 2015;7(02):198–203

37 Watterson SH, Liu Q, Beaudoin Bertrand M, et al. Discovery of Branebrutinib (BMS-986195): a strategy for identifying a highly potent and selective covalent inhibitor providing rapid in vivo inactivation of Bruton's tyrosine kinase (BTK). J Med Chem 2019; 62(07):3228–3250

38 Yang B, Vasbinder MM, Hird AW, et al. Adventures in scaffold morphing: discovery of fused ring heterocyclic checkpoint kinase 1 (CHK1) inhibitors. J Med Chem 2018;61(03):1061–1073

39 Hicken EJ, Marmsater FP, Munson MC, et al. Discovery of a novel class of imidazo[1,2-a]pyridines with potent PDGFR activity and oral bioavailability. ACS Med Chem Lett 2013;5(01):78–83

40 Zhang X, Mao J, Wei M, Qi Y, Zhang JZH. HergSPred: accurate classification of hERG blockers/nonblockers with machine-learning models. J Chem Inf Model 2022;62(08):1830–1839

41 Asahi Y, Nomura F, Abe Y, et al. Electrophysiological evaluation of pentamidine and 17-AAG in human stem cell-derived cardiomyocytes for safety assessment. Eur J Pharmacol 2019;842:221–230

42 Sharifi M. Computational approaches to understand the adverse drug effect on potassium, sodium and calcium channels for predicting TdP cardiac arrhythmias. J Mol Graph Model 2017;76:152–160

43 Blum CA, Zheng X, De Lombaert S. Design, synthesis, and biological evaluation of substituted 2-cyclohexyl-4-phenyl-1H-imidazoles: potent and selective neuropeptide Y Y5-receptor antagonists. J Med Chem 2004;47(09):2318–2325

44 Rampe D, Wible B, Brown AM, Dage RC. Effects of terfenadine and its metabolites on a delayed rectifier K+ channel cloned from human heart. Mol Pharmacol 1993;44(06):1240–1245

45 Ganellin R, Roberts S, Jefferies R. Introduction to Biological and Small Molecule Drug Research and Development: Theory and Case Studies. Amsterdam: Academic Press; 2013

46 Tschirhart JN, Zhang S. Fentanyl-induced block of hERG channels is exacerbated by hypoxia, hypokalemia, alkalosis, and the presence of hERG1b. Mol Pharmacol 2020;98(04):508–517

47 Uko NE, Güner OF, Matesic DF, Bowen JP. Akt pathway inhibitors. Curr Top Med Chem 2020;20(10):883–900

48 Dong X, Zhan W, Zhao M, et al. Discovery of 3,4,6-trisubstituted piperidine derivatives as orally active, low hERG blocking Akt inhibitors via conformational restriction and structure-based design. J Med Chem 2019;62(15):7264–7288

49 Reck F, Alm RA, Brassil P, et al. Novel N-linked aminopiperidine inhibitors of bacterial topoisomerase type II with reduced pK(a): antibacterial agents with an improved safety profile. J Med Chem 2012;55(15):6916–6933

50 Zaman MA, Oparil S, Calhoun DA. Drugs targeting the renin-angiotensin-aldosterone system. Nat Rev Drug Discov 2002;1 (08):621–636

51 Skeggs LT Jr, Kahn JR, Lentz K, Shumway NP. The preparation, purification, and amino acid sequence of a polypeptide renin substrate. J Exp Med 1957;106(03):439–453

52 Ehara T, Irie O, Kosaka T, et al. Structure-based design of substituted piperidines as a new class of highly efficacious oral direct Renin inhibitors. ACS Med Chem Lett 2014;5(07):787–792

53 Gao Y, Zhao X, Sun X, et al. Enantioselective detection, bioactivity, and degradation of the novel chiral fungicide oxathiapiprolin. J Agric Food Chem 2021;69(11):3289–3297

54 Saha D, Kharbanda A, Yan W, Lakkaniga NR, Frett B, Li HY. The exploration of chirality for improved druggability within the human kinome. J Med Chem 2020;63(02):441–469

55 Feng PF, Zhang B, Zhao L, et al. Intracellular mechanism of rosuvastatin-induced decrease in mature hERG protein expression on membrane. Mol Pharm 2019;16(04):1477–1488